Self-Assembly at High Pressures: SANS Study of the Effect of Pressure on Microstructure of C8E5 Micelles in Water

ARTICLE *in* INDUSTRIAL & ENGINEERING CHEMISTRY · AUGUST 2003

DOI: 10.1021/ie0302387

7 AUTHORS, INCLUDING:

Mark A Mchugh
Virginia Commonwealth University
194 PUBLICATIONS **4,919** CITATIONS
SEE PROFILE

John H. van Zanten
North Carolina State University
69 PUBLICATIONS **1,975** CITATIONS
SEE PROFILE

Michael Paulaitis
Johns Hopkins Medicine
165 PUBLICATIONS **4,759** CITATIONS
SEE PROFILE

Self-Assembly at High Pressures: SANS Study of the Effect of Pressure on Microstructure of C_8E_5 Micelles in Water

M. Lesemann,[†] H. Nathan,[‡] T. P. DiNoia,[§] C. F. Kirby,[||] M. A. McHugh,[⊥] J. H. van Zanten,[#] and M. E. Paulaitis*

Department of Chemical Engineering, The Johns Hopkins University, Baltimore, Maryland 21218

We present the results of a high-pressure small-angle neutron scattering study of the effect of pressure on surfactant microstructure. The study was carried out on a solution of 1 wt % C_8E_5 in D_2O at 29.4 °C and pressures up to 310 MPa. The C_8E_5 micelles that form under these conditions are noninteracting. We find that applying pressure leads to a pronounced decrease in the micelle radius of gyration and the forward scattering intensity over the pressure range from ambient to 150 MPa. The partial molecular volume of the surfactant and the extent of hydration of the surfactant head groups in the micelle were also determined using the method of solvent contrast variation. Both quantities decrease with the application of pressure up to 150 MPa. Core−shell model fits to the scattering spectra over the entire *q*-range indicate that the shell radius decreases, while the hydrophobic core radius increases slightly with pressure. The pressure dependence of the shell radius is notably similar to that observed for the radius of gyration. Collectively, these observations lead to the conclusion that the effect of pressure on C_8E_5 micellization is to induce the dehydration of surfactant head groups and the collapse of the hydrophilic micelle shell at pressures between ambient and 150 MPa.

Introduction

Nonionic surfactants of the type C_iE_j (*n*-alkyl polyoxyethylene ether) form a variety of microstructures in water, ranging from simple micelles at low surfactant concentrations to complex mesophases, such as hexagonal or lamellar phases, at high concentrations.[1,2] The formation of these microstructures has been studied as a function of temperature, the hydrophobic−lipophobic balance of the amphiphile, and the addition of alkanes, salts, or ionic cosurfactants. However, the effect of pressure on microstructure has not been studied as extensively. Our motivation for exploring this pressure dependence is to assess the use of pressure as an independent thermodynamic variable to control surfactant self-assembly. An advantage of applying pressure to stabilize certain microstructures would be to effectively uncouple self-assembly from other thermodynamic variables in processes where the microstructure is used as a template, for example, in the fabrication of nanostructured materials.

In general, small-angle neutron scattering (SANS) is particularly well-suited for accurate measurements of surfactant microstructures because the range of length scales probed includes both the particle size and the interparticle spacing. The effect of pressure on microstructure observed in SANS measurements[3−6] is a manifestation of the geometric packing constraints that govern microstructure formation and stability.[7] For example, recent high-pressure SANS experiments to measure microstructure in a solution of pentaethylene glycol mono-*n*-dodecyl ether ($C_{12}E_5$) in D_2O revealed a pressure-induced transition from a network of branched, threadlike micelles to hexagonally ordered bundles of cylindrical micelles.[8] The instability of this network at elevated pressures was predicted from an analysis of the geometric packing constraints on the branch points, which showed that these branch points, and hence the network, become unstable with the application of pressure. The hydrophobic micelle core also freezes at elevated pressures, which leads to the formation of ordered bundles of cylindrical micelles. The significance of this finding is to show that pressure can be used to direct self-assembly to obtain certain microstructures in aqueous solutions that are virtually impossible to obtain by changing temperature.

Here, we report the results of high-pressure SANS experiments to study the effect of pressure on microstructure in a solution of 1.0 wt % pentaethylene glycol monooctyl ether (C_8E_5) surfactant micelles in water at 29.4 °C and pressures up to 310 MPa. At this temperature and surfactant concentration, a single-phase micellar solution forms at ambient pressure, well below the lower critical solution temperature (LCST) for liquid−liquid equilibrium,[9] and far removed from the critical micelle concentration (cmc) of C_8E_5 in D_2O at much lower surfactant concentrations.[10] The C_8E_5 micelles are roughly spherical, monodisperse, and noninteracting at these conditions.[11,12] Applying pressure shifts the LCST to higher temperatures,[13] and raises the cmc to a maximum of 0.33 wt % C_8E_5 at ∼150 MPa. The cmc decreases with pressure above 150 MPa.[10]

Experimental Section

Scattering experiments were performed on the NG-7 30 m SANS instrument at the NIST Center for Neutron

* To whom correspondence should be addressed.
[†] Current address: W. R. Grace, Columbia, MD.
[‡] Current address: Johns Hopkins School of Medicine, Baltimore, MD.
[§] Current address: Grace Performance Chemicals, Cambridge, MA.
[||] Current address: Northrop Grumman Corp., Baltimore, MD.
[⊥] Current address: Department of Chemical Engineering, Virginia Commonwealth University, Richmond, VA.
[#] Current address: Department of Chemical Engineering, North Carolina State University, Raleigh, NC.

10.1021/ie0302387 CCC: $25.00
Published on Web 08/20/2003

Research in Gaithersburg, MD. Neutrons of wavelength $\lambda = 6$ Å with a distribution of $\Delta\lambda/\lambda = 15\%$ were incident on samples held in a custom-built high-pressure SANS cell. The intensity of elastically scattered neutrons, $I(q)$, was measured as a function of the magnitude of the scattering vector, $q = (4\pi/\lambda)\sin(\theta/2)$, over the range $0.02 \leq q/\text{Å}^{-1} \leq 0.30$. Sample scattering was corrected for background and empty cell scattering, and the sensitivity of individual detector pixels was normalized. Corrected data sets were circularly averaged and placed on an absolute scale using standard samples and software supplied by NIST.[14] Instrumental smearing was simulated[15] for the instrument configurations used, eliminating smeared data points from the combined data set.

The custom-built high-pressure SANS cell consists of a stainless steel outer cell, rated to 4 kbar, and an inner cell containing the surfactant solution. The design of this high-pressure cell is described in detail elsewhere.[16,17] A unique feature of the cell design is to isolate the sample from the pressurizing fluid and the metal walls of the outer cell by enclosing it in the inner cell. This inner cell consists of a flexible Teflon sleeve that fits tightly around the two sapphire windows of the outer cell such that the sample path length (i.e., the distance between the windows) is 1.00 mm at atmospheric pressure. The change in path length due to deformation of the high-pressure cell at elevated pressures was accounted for based on an independent calibration of this deformation.[16]

Temperature was controlled using a constant-temperature bath provided by NIST (±0.01 °C sensitivity) that circulated ethylene glycol through the aluminum jacket that held the high-pressure cell. Temperature was measured with an Omega E-type thermocouple and meter (±0.5 °C accuracy). The stability of temperature readings during an experiment was ±0.1 °C. Pressure was generated manually using a pressure generator and measured at the cell using a Viatran Model 345 transducer (0−60,000 psi, <±60 psi nonlinearity) and meter (±1 psi sensitivity).

C_8E_5 (>97% purity) was purchased from Bachem Bioscience and used without further purification. D_2O (99.9% purity) was purchased from Aldrich Chemicals. The surfactant was apportioned into 2.5-mL aliquots in a glovebox and then stored at −15 °C until used. Aqueous solutions of 1 wt % C_8E_5 were prepared by weight and allowed to equilibrate overnight at room temperature.

Results and Discussion

Scattering spectra measured at 29.4 °C and representative pressures of 4, 69, 138, and 310 MPa are shown in Figure 1. At low q, the spectra can be fit using the Guinier approximation,

$$I(q) = I(0)\exp(-{}^1/_3 R_g{}^2 q^2) \qquad (1)$$

where R_g is the radius of gyration of the micelle and $I(0)$ is the scattering intensity at $q = 0$. These results are shown in Figure 2. In each case, a linear plot of $\ln[I(q)]$ vs q^2 was obtained for $q \leq 0.01$ Å^{-1}; R_g and $I(0)$ calculated from the slope and $q = 0$ intercept, respectively, are shown in Figure 3.

At 4 MPa, $R_g = 19.77 \pm 0.03$ Å, which corresponds to a micelle radius of 25.5 Å for a spherical micelle with uniform scattering properties. This micelle radius is in good agreement with values obtained from independent

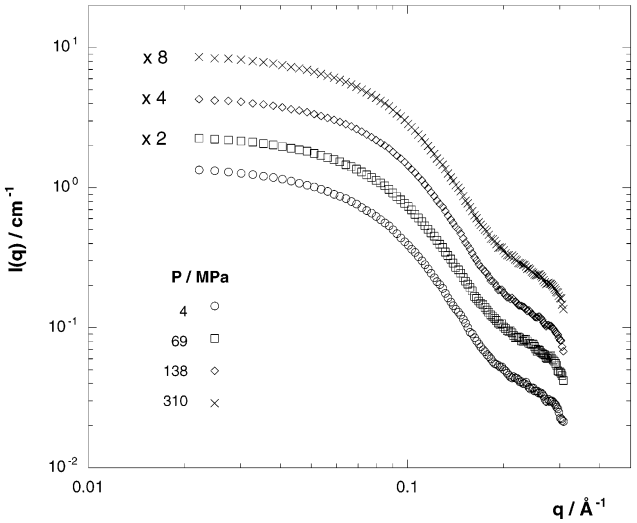

Figure 1. Measured scattering intensities as a function of the magnitude of the scattering wave vector for a solution of 1 wt % C_8E_5 in D_2O at 29.4 °C and pressures of 4, 69, 138, and 310 MPa. The spectra at the three higher pressures have been offset by factors indicated on the figure.

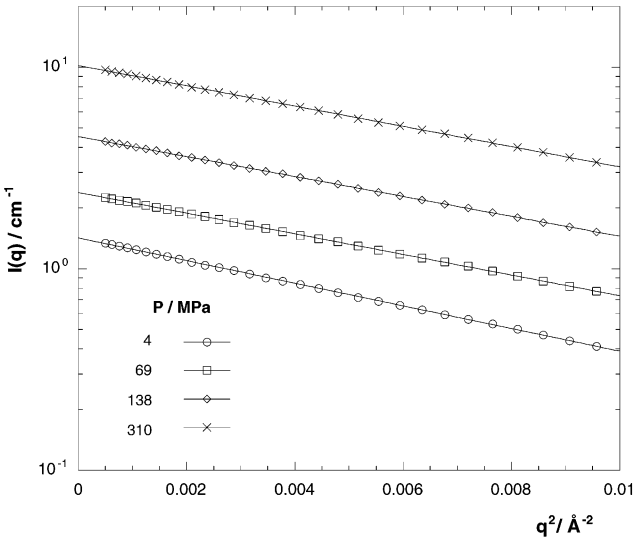

Figure 2. Guinier plots of the measured scattering spectra in Figure 1.

SANS measurements of the C_8E_5 micelle radius in D_2O at the same conditions: 23.5 ± 0.15 Å [12] and 25.5 ± 0.10 Å.[18] The latter value was determined by fitting $I(q)$ over the entire q-range using a model for noninteracting, monodisperse hard spheres. A slightly smaller radius of ∼22 Å was observed in a molecular dynamics (MD) simulation of the C_8E_5 micelle in water.[19] The application of pressure up to ∼150 MPa reduces R_g, which then increases slightly with pressure at higher pressures up to 310 MPa. Values for R_g derived from the SANS spectra using the pair distance distribution function[20] (not shown) show a similar pressure dependence up to ∼150 MPa, but are constant at higher pressures. These values are also shifted down by ∼1 Å across the entire range of pressures compared to those obtained from the Guinier analysis. The pair distance distribution functions also vanish at values greater than the length of a fully extended surfactant molecule, indicating that the micelles have on average a slightly nonspherical shape. A globular, but slightly ellipsoidal shape was noted in the MD simulation of the C_8E_5 micelle in water.[19]

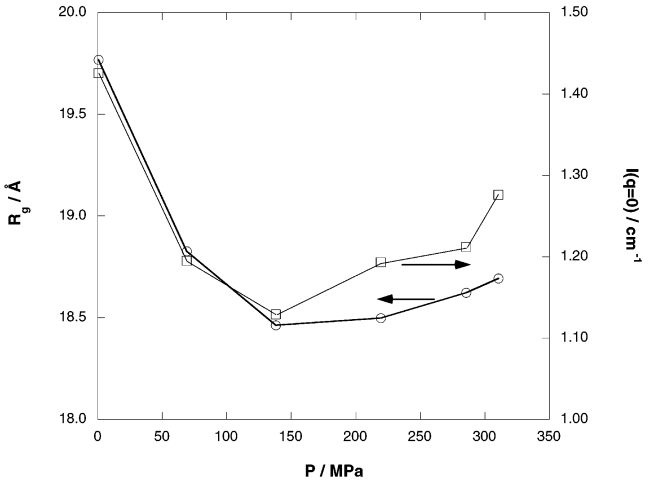

Figure 3. Pressure dependence of the radius of gyration (open circles) and the forward scattering intensity (open squares) obtained from a Guinier analysis (eq 1) of the measured scattering intensity as a function of the magnitude of the scattering wave vector for a solution of 1 wt % of C_8E_5 in D_2O at 29.4 °C.

The effect of pressure on $I(0)$ (Figure 3) is notably similar to that obtained for R_g and can be attributed to the pressure dependence of the cmc, the micelle aggregation number, N_{agg}, and the partial molecular volume of the surfactant, $\bar{v}_s$:[21]

$$I(0) = \frac{(c - \text{cmc})}{N_{agg}}[N_{agg}(b_s - \bar{v}_s\rho^\circ)]^2 \qquad (2a)$$

$$= (c - \text{cmc})N_{agg}(b_s - \bar{v}_s\rho^\circ)^2 \qquad (2b)$$

where $(c - \text{cmc})$ is the surfactant concentration in excess of the cmc and $(c - \text{cmc})/N_{agg}$ is the concentration of micelles (scattering particles) in solution. The contrast in scattering for a single micelle relative to the solvent is given by N_{agg} times the difference in scattering lengths of a surfactant molecule, b_s, and a solvent molecule that would occupy the same volume; that is, the product of $\bar{v}_s$ and the scattering length density of the solvent, ρ°. The pressure dependence of the cmc has been measured for C_8E_5 in D_2O at 30 °C by ^1H NMR chemical shifts[10] and, thus, can be accounted for by defining the forward scattering intensity relative to the surfactant concentration in excess of the cmc,

$$I'(0) \equiv \frac{I(0)}{(c - \text{cmc})} = N_{agg}(b_s - \bar{v}_s\rho^\circ)^2 \qquad (3)$$

which gives the effect of pressure on $I'(0)$ in terms of the pressure dependence of N_{agg} and $\bar{v}_s$. These quantities and their pressure dependence can, in principle, be evaluated using the method of solvent contrast variation[21] at each pressure of interest.

The method of solvent contrast variation involves systematically adjusting the scattering length density of the solvent by preparing solvent mixtures of D_2O and H_2O. Thus,

$$\rho^\circ = x\rho_{D_2O} + (1 - x)\rho_{H_2O} \qquad (4)$$

where x is the fraction of D_2O in the solvent and ρ_i is the scattering length density of component i. The scattering length densities of D_2O and H_2O are at opposite extremes of the range of scattering length densities of most molecules. Thus, an advantage of the method is that solvent mixtures of D_2O and H_2O can be prepared to match the scattering contrast of almost any molecule of interest. It follows from eqs 3 and 4 that $\bar{v}_s$ and N_{agg} can be obtained from the slope and $\rho^\circ = 0$ intercept of a plot of $\sqrt{I'(0)}$ vs x. These plots are shown in Figure 4 for four representative pressures; $\bar{v}_s$ at each pressure, obtained from the slope, is given in Table 1. At 4 MPa, $\bar{v}_s = 596$ Å^3/molecule, in good agreement with $\bar{v}_s = 575$ Å^3/molecule, calculated assuming additive specific volumes for the surfactant head and tail groups.[22] The plots at the three higher pressures essentially superimpose, such that $\bar{v}_s = \sim 350-370$ Å^3/molecule, independent of pressure.

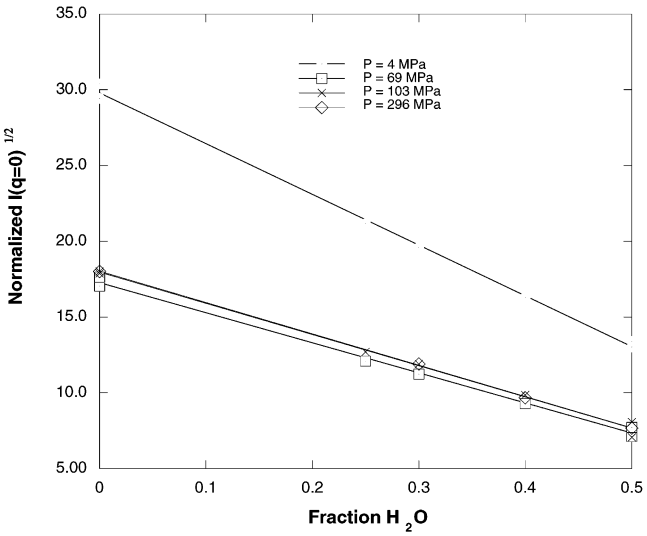

Figure 4. Square root of the forward scattering intensity as a function of the fraction of H_2O in the D_2O:H_2O solvent mixture at 29.4 °C and pressures of 4, 69, 103, and 296 MPa. The $I(0)$ are normalized by the forward scattering intensity at the match point for C_8E_5 micelles in D_2O:H_2O mixtures (H_2O fraction ~ 0.92).

Table 1. Surfactant Partial Molecular Volumes and the Number of Hydration Water Molecules per Surfactant Molecule in the C_8E_5 Micelle at 29.4 °C Derived from the Solvent Contrast Variation Experiments at the Four Pressures in Figure 4

P (MPa)	$\bar{v}_s$ (Å^3/molecule)	$\alpha \equiv N_{D_2O}/N_{agg}$
4	596	15
69	368	1
103	369	1
296	353	1

A determination of N_{agg} requires the $\rho^\circ = 0$ intercept, which is typically located by interpolating measurements made at D_2O:H_2O compositions well above and below the solvent composition corresponding to $\rho^\circ = 0$, the so-called match point. However, the match point for C_8E_5 in D_2O:H_2O mixtures at ambient pressure is located at $x \sim 0.09$, which precludes such an interpolation. An accurate extrapolation could be contemplated, but would require measurements at a much larger number of D_2O compositions well above the match point. Since this approach is not feasible for the full range of pressures of interest, an accurate determination of N_{agg} and its pressure dependence using the method of solvent contrast variation was not pursued for this surfactant solution.

As noted above, however, the pressure dependence of $I'(0)$ is similar to that obtained for R_g, which can also

be defined in terms of N_{agg} and $\bar{v}_s$,

$$c_1 R_g^{\ 3} = N_{agg}\bar{v}_s + N_{D_2O}\bar{v}_{D_2O} \quad (5a)$$

$$= N_{agg}(\bar{v}_s + \alpha\bar{v}_{D_2O}) \quad (5b)$$

where c_1 is a geometric constant, N_{D_2O} is the number of water molecules in the micelle, $\bar{v}_{D_2O}$ is the partial molecular volume of water, and $\alpha \equiv N_{D_2O}/N_{agg}$ is the number of water molecules per surfactant molecule in the micelle. Combining eqs 3 and 5b to eliminate N_{agg} gives

$$\frac{c_1 R_g^{\ 3}}{I'(0)} = \frac{\bar{v}_s + \alpha\bar{v}_{D_2O}}{(b_s - \bar{v}_s\rho^\circ)^2} \quad (6)$$

which provides a relationship for determining the extent of hydration of the C_8E_5 surfactant in the micelles through the parameter, α. The calculation of α is based on two assumptions: the micelles are spherical with uniform scattering properties, which defines $c_1 = (4\pi/3)(5/3)^{3/2}$, and the molecular volume for pure liquid D_2O is a reasonable approximation for $\bar{v}_{D_2O}$. The values of α calculated using eq 6 are given in Table 1. At 4 MPa, α is ~15, which corresponds to 3 water molecules per surfactant EO group if, as expected, water hydrates the hydrophilic micelle shell, but does not penetrate the hydrophobic core.[19] This value is in good agreement with a hydration number of 2−3 water molecules per monomer of poly(ethylene oxide) (PEO) at ambient conditions.[23−25] The PEO monomer is an analogue for the EO groups of C_8E_5. The value of ~15 is also in good agreement with the number of water molecules per surfactant molecule obtained from MD simulation of the C_8E_5 micelle in water.[19]

At all three higher pressures, α decreases to ~1. This pronounced decrease in α, and the concomitant decreases in $\bar{v}_s$ and R_g with increasing pressure, suggest a pressure-induced dehydration of the surfactant head groups and a collapse of the hydrophilic micelle shell. The phenomenon is reminiscent of the pressure-induced crossover from good to poor solvent behavior for PEO in water reflected in measurements of lower LCSTs for PEO−water mixtures at high pressures,[26,27] and in SANS measurements on PEO−water mixtures that show R_g for PEO decreases with increasing pressure.[28] A collapse of PEO chains tethered to spherical poly(*N*-isopropylacrylamide) microgels has also been observed in experiments where the collapse is induced by an increase in the PEO grafting density.[29,30] The higher grafting density is thought to exclude water molecules from the PEO layer, causing the chains collapse as the number of excluded water molecules becomes large.

Information on the internal structure of the micelle can be obtained by fitting a standard core−shell model to $I(q)$ over the entire q-range.[21] This core−shell description was selected over a simple, spherical micelle with uniform scattering properties because the scattering length of the C_8E_5 head group is $+2.273 \times 10^{-12}$ cm^{-2}, while the scattering length of the tail group is -1.043×10^{-12} cm^{-2}, and previous work [31] has shown that even a low-resolution description of $I(q)$ requires at least a two-shell model for a micelle with opposite signs of the contrast for the core and shell. In the context of the core−shell model, the micelles consist of a spherical hydrophobic core having a uniform scattering length density, ρ_c, surrounded by a spherical hydrophilic shell with a different, but likewise uniform scattering length density, ρ_{sh}. The scattered intensity given by the core−shell model is

$$\frac{I(q)}{I(0)} = \left(x\frac{3j_1(qR_c)}{qR_c} + (1-x)\frac{3j_1(qR_{sh})}{qR_{sh}}\right)^2 \quad (7)$$

where R_c and R_{sh} are the core and shell radii, respectively, j_1 is the first-order Bessel function, and

$$x = \frac{R_c^{\ 3}(\rho_c - \rho_{sh})}{R_c^{\ 3}(\rho_c - \rho_{sh}) + R_{sh}^{\ 3}(\rho_{sh} - \rho^\circ)} \quad (8)$$

is the contribution to $I(q)$ due to scattering from the micelle core in excess of that from a micelle with a uniform scattering length density corresponding to ρ_{sh}. Using $I(0)$ from the Guinier analysis, the scattering spectra were fit to eq 7 with R_c, R_{sh}, and x as adjustable parameters. Excellent fits were obtained at all conditions as illustrated in Figure 5 for spectra at two representative pressures. The parameters obtained from the fits are given in Table 2. As expected, attempted fits of the spectra assuming spherical micelles with a uniform scattering length density produced much different and less accurate descriptions, especially at high q. Radii of gyration calculated using these fitted parameters were also found to be within 1.5% of those values obtained directly from the Guinier analysis. The fits of R_g from the Guinier analysis at low q will be most sensitive to the values of R_{sh}, while the fits of $I(q)$ at

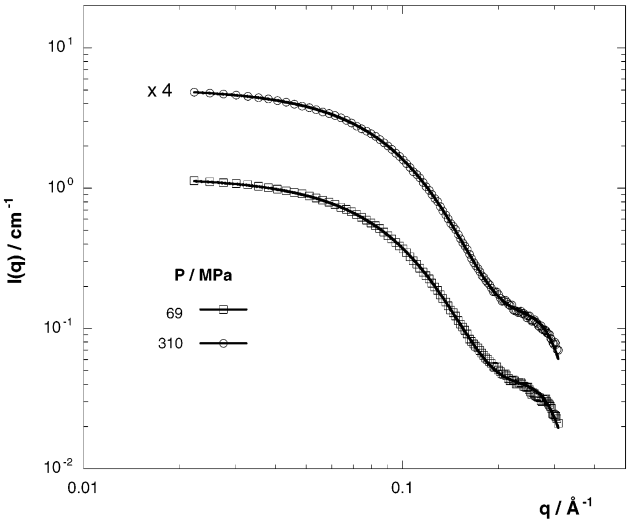

Figure 5. Core−shell model fits (eq 7) to the measured scattering intensities as a function of the magnitude of the scattering wave vector for a solution of 1 wt % C_8E_5 in D_2O at 29.4 °C and pressures of 69 and 310 MPa. The spectrum at 310 MPa has been offset by a factor of 4 as indicated on the figure.

Table 2. Parameters from the Core−Shell Model Fits (eq 7) of the Measured Scattering Intensities as a Function of the Magnitude of the Scattering Wave Vector for a Solution of 1% by Weight C_8E_5 in D_2O at 29.4 °C[a]

P (MPa)	R_c (Å)	R_{sh} (Å)	x
69	10.80	30.66	0.414
138	10.90	30.00	0.409
220	10.98	29.86	0.407
296	11.19	29.89	0.407
310	11.20	29.88	0.401

[a] See Figure 5. The estimated uncertainities in these parameters are ±0.018 Å for R_c, ±0.026 Å for R_{sh}, and ±0.001 for x.

high q will be more sensitive to the value of R_c. Thus, accurate descriptions of both R_g and $I(q)$ indicate that the values obtained for R_c and R_{sh} are reasonable. The range of values obtained for R_c (10.8−11.2 Å) is also reasonable based on a predicted maximum chain length for the C_8 hydrocarbon tail group of 11.6 Å,[7] and the observation that the C_8 hydrocarbon chains in the C_8E_5 micelle adopt liquid *n*-octane-like, extended conformations at ambient pressure.[19]

We note, however, that the values of x in Table 2 imply a much higher ρ_{sh} than expected, based on the scattering length densities of the C_8E_5 head group and D_2O with the extent of C_8E_5 head group hydration calculated using the values of α in Table 1. Convergence to these high values was notably robust, even with initial values of $x \sim 0$. A similar observation was made in a SANS study of micelles formed by poly(ethylene-*co*-propylene)−PEO block copolymers in water and was attributed to a much higher density of waters hydrating the PEO chains of the micelles.[32] The extent of hydration of the surfactant head groups in the C_8E_5 micelle calculated using the values of x in Table 2 is, however, about 1 order of magnitude too high to be physically realistic. An alternative interpretation is that the unusually high values of x reflect limitations in the core−shell model that can be attributed to the assumption of spherical symmetry. As noted above, the pair distance distribution functions that were calculated from the scattering spectra and the MD simulation of the C_8E_5 micelle in water both indicate a globular, but not perfectly spherical micelle. A core−shell model that accounts for nonspherical shapes will have additional fitting parameters and, as such, would require additional information in the form of either independent experimental data or molecular simulations to validate them, which is beyond the scope of the current study. Therefore, in the context of the core−shell model that was used here, we accept the parameter x as simply a fitting parameter without a physical interpretation.

The fitted values for R_c and R_{sh} are plotted as a function of pressure in Figure 6. The pressure dependence of R_{sh} tracks almost quantitatively with that of R_g, while R_c increases slightly with increasing pressure. The decrease in R_{sh} with increasing pressure is also much more abrupt than the increase in R_c, which is nearly linear with pressure. These observations provide further support for a pressure-induced collapse of the micelle shell. It should also be noted that the increase in R_c with increasing pressure is counter-intuitive. On the basis of the compressibility of pure liquid *n*-octane at 29.4 °C, we would expect the hydrophobic micelle core to compress slightly under pressure.[33] Expansion of the core could be a manifestation of the intercalation of surfactant EO groups into the interfacial region as the shell collapses. This hypothesis is supported by the MD simulation of the C_8E_5 micelle in water where it was found that the surfactant head groups adopt on average partially coiled, nonlinear chain conformations in contrast to the C_8 hydrocarbon chains, which adopt on average liquid *n*-octane-like, extended conformations.[19] Thus, the folding back and penetration of these relatively long and flexible head groups into the interfacial region of the micelle as the shell dehydrates with increasing pressure appears to be feasible. A resolution of the molecular origins of this observation is, however, beyond the scope of the primitive core−shell model that was used to fit our scattering spectra. Using the structural details obtained from MD simulations of individual C_8E_5 micelles in water at elevated pressures as a basis for analyzing these spectra would provide a molecularly unambiguous description of $I'(0)$. This molecularly detailed approach to modeling SANS spectra is currently in progress.

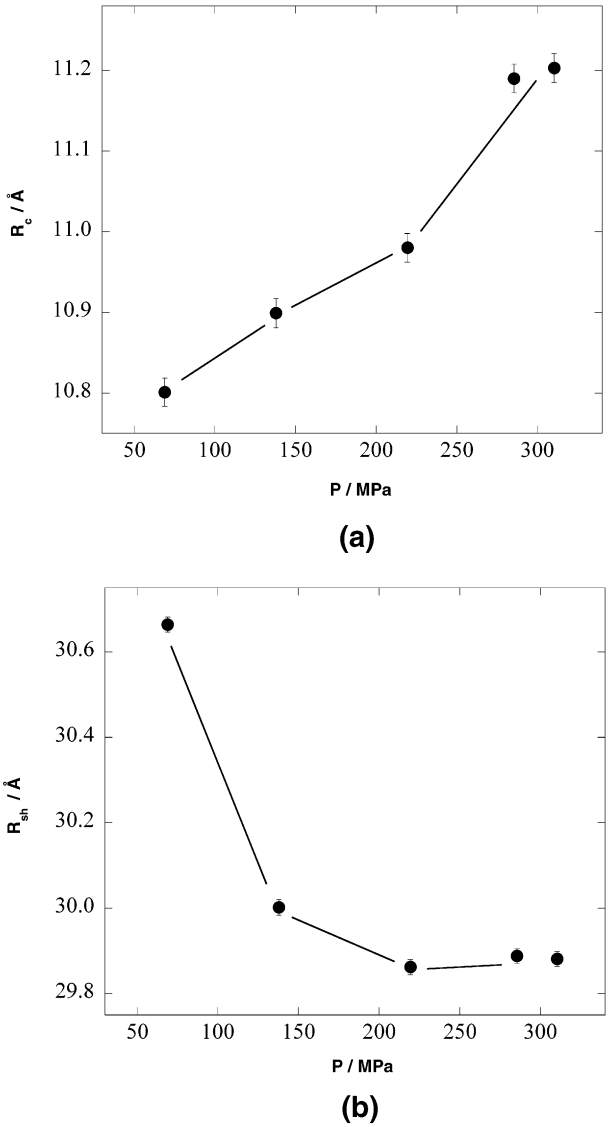

Figure 6. (a) Pressure dependence of the C_8E_5 micelle core radius at 29.4 °C derived from the core−shell model fits of the scattering spectra. (b) Pressure dependence of the C_8E_5 micelle shell radius at 29.4 °C derived from the core−shell model fits of the scattering spectra.

Conclusions

Our study of the effect of pressure on C_8E_5 micellization in D_2O has shown that the application of pressure induces the dehydration of the surfactant head groups, which leads to the collapse of the hydrophilic micelle shell. This conclusion is based on several findings. We found that increasing pressure leads to a pronounced decrease in the micelle radius of gyration. A similar pressure dependence was observed for the scattering intensity at $q = 0$. Using the method of solvent contrast variation, we determined the partial molecular volume of the surfactant and the extent of hydration of the surfactant head groups and found that these quantities decrease with the application of pressure. The pressure dependence in both cases is similar to that observed for

the radius of gyration. From core−shell model fits to $I(q)$ over the entire q-range, we determined that the micelle shell collapses, while the core expands slightly with increasing pressure. Moreover, the pressure dependence of the shell radius is notably similar to that for the radius of gyration. The pronounced decrease in the shell radius is in contrast to the nearly linear increase in the core radius with increasing pressure. The expansion of the micelle hydrophobic core was unexpected, and the molecular origins of this observation have yet to be resolved.

Finally, this dilute aqueous solution of nonionic C_8E_5 micelles was selected as a model system for this study for two reasons: interparticle interactions could be neglected and, more importantly, the surfactant microstructure at ambient pressure is well-known and simple. Our results establish that the microstructure for this surfactant system is sensitive to pressure; significant changes in core−shell structure of the micelle can be brought about with the application of pressures on the order of 150 MPa. Recent studies of the effects of pressure on incrementally more complex systems—for example, $C_{12}E_5$ in water[8]—reveal changes in microstructure that are unique to pressure. We believe that further studies of surfactant self-assembly at high pressure are likely to lead to more discoveries of pressure effects that give rise to structures and structural transitions that have not been anticipated and that may have interesting practical applications.

Acknowledgment

Financial support from the National Science Foundation (CHE-95-26273) and the National Aeronautics and Space Administration (NAG3-1954) are gratefully acknowledged. This work is based upon activities supported by the National Science Foundation under agreement No. DMR-9986442. Trade names mentioned do not imply endorsement by NIST.

Literature Cited

(1) Strey, R. Water-Nonionic Surfactant Systems, and the Effect of Additives. *Ber. Bunsen-Ges. Phys. Chem.* **1996**, *100*, 182.

(2) Strey, R.; Schomäcker, R.; Roux, D.; Nallet, F.; Olsson, U. Dilute Lamellar and L_3 Phases in the Binary Water $C_{12}E_5$ System. *J. Chem. Soc., Faraday Trans.* **1990**, *86*, 2253.

(3) Gorski, N.; Kalus, J.; Schwahn, D. Pressure Dependence of the Chemical Potential of Tetradecyldimethylaminoxide Micelles in D_2O. A SANS Study. *Langmuir* **1999**, *15*, 8080 and references therein.

(4) Steytler, D. C.; Holmes, J. D. Aggregation and solubilisation in near critical CO_2 studied by scattering methods. *Curr. Opin. Colloid Interface Sci.* **1998**, *3*, 299 and references therein.

(5) Nagao, M.; Seto, H. Small-angle neutron scattering study of a pressure-induced phase transition in a ternary microemulsion composed of AOT, D_2O, and *n*-decane. *Phys. Rev. E* **1999**, *59*, 3169 and references therein.

(6) Eastoe, J.; Steytler, D. C.; Robinson, B. H.; Heenan, R. K. Pressure-Induced Structural Changes in Water-in-Propane Microemulsions. *J. Chem. Soc., Faraday Trans. 1* **1994**, *90*, 3121 and references therein.

(7) Israelachvili, J. N.; Mitchell, D. J.; Ninham, B. W. Theory of Self-Assembly of Hydrocarbon Amphiphiles into Micelles and Bilayers. *J. Chem. Soc., Faraday Trans. 1* **1976**, *72*, 1525.

(8) Bosssev, D. P.; Kline, S. R.; Israelachvili, J. N.; Paulaitis, M. E. Pressure-Induced Freezing of the Hydrophobic Core Leads to a $L_1 \rightarrow H_1$ Phase Transition for $C_{12}E_5$ Micelles in D_2O. *Langmuir* **2001**, *17*, 7728.

(9) Schubert, K.-V.; Strey, R.; Kahlweit, M. J. A new purification technique for alkyl polyglycol-ethers and micscibility gaps for water C_iE_j. *J. Colloid Interface Sci.* **1991**, *141*, 21.

(10) Lesemann, M.; Thirumoorthy, K.; Kim, Y. J.; Jonas, J.; Paulaitis, M. E. Pressure Dependence of the Critical Micelle Concentration of a Nonionic Surfactant in Water Studied by ^1H NMR. *Langmuir* **1998**, *14*, 5339.

(11) Zulauf, M.; Rosenbusch, J. P. Micelle Clusters of Octylhydroxyoligo(oxyethylenes). *J. Phys. Chem.* **1983**, *87*, 856.

(12) Hayter, J. B.; Zulauf, M. Attractive interactions in critical scattering from nonionic micelles. *Colloid Polym. Sci.* **1982**, *260*, 1023.

(13) Nishikido, N.; Yoshimura, N.; Tanaka, M.; Kaneshina, S. Effect of Pressure on the Solution Behavior of Nonionic Surfactants in Water. *J. Colloid Interface Sci.* **1980**, *78*, 338.

(14) NIST SANS Data Reduction and Imaging Software, 1998.

(15) Barker, J. G.; Pedersen, J. S. Instrumental smearing effects in radially symmetrical small-angle neutron-scattering by numerical and analytical methods. *J. Appl. Crystallogr.* **1995**, *28*, 105.

(16) Ferdinand, S. Pressure-Induced Changes in Microstructure of Oil-In−Water Microemulsions. M. S. Thesis, Johns Hopkins University, Baltimore, MD, 2000.

(17) DiNoia, T. P.; Kirby, C. F.; van Zanten, J. H.; McHugh, M. A. SANS study of polymer-supercritical fluid solutions: Transitions from liquid to supercritical fluid solvent quality. *Macromolecules* **2000**, *33*, 6321.

(18) Bossev, D. P. NIST Center for Neutron Research, private communication, 2002.

(19) Garde, S.; Yang, L.; Dordick, J. S.; Paulaitis, M. E. Molecular dynamics simulation of C_8E_5 micelle in explicit water: structure and hydrophobic solvation thermodynamics. *Mol. Phys.* **2002**, *100*, 2299.

(20) Svergun, D. I. Mathematical Methods in Small-Angle Scattering Data Analysis. *J. Appl. Crystallogr.* **1991**, *24*, 485.

(21) Chen, S. H. Small Angle Neutron Scattering Studies of the Structure and Interaction in Micellar and Microemulsion Systems. *Annu. Rev. Phys. Chem.* **1986**, *37*, 351.

(22) Kaneshina, S.; Yoshimoto, M.; Kobayashi, H.; Nishikido, N.; Sugihara, G.; Tanaka, M. Effect of Pressure on Apparent Molal Volumes of Nonionic Surfactants in Aqueous Solutions. *J. Colloid Interface Sci.* **1980**, *73*, 124.

(23) Graham, N. B.; Zulfiqar, M.; Mwachuku, N. E.; Rashid, A. Interaction of poly(ethylene oxide) with solvents: 2. Water-poly(ethylene glycol). *Polymer* **1989**, *30*, 528.

(24) Liu, K.-J.; Parsons, J. L. Solvent effects on preferred conformation of poly(ethylene glycols). *Macromolecules* **1969**, *2*, 529.

(25) Bell, W.; Pethrick, R. A. Adiabatic Compressibility of Polymer-Solutions. *Eur. Polym. J.* **1972**, *8*, 927.

(26) Cook, R. L.; King, H. E.; Peiffer, D. G. Pressure-Induced Crossover from Good to Poor Solvent Behavior for Polyethylene Oxide in Water. *Phys. Rev. Lett.* **1992**, *69*, 3072.

(27) Hammouda, B.; Ho, D.; Kline, S. SANS from Poly(ethylene oxide)/Water Systems. *Macromolecules* **2002**, *35*, 8578.

(28) Vennemann, N.; Lechner, M. D.; Oberthür, R. C. Thermodynamics and conformation of polyoxyethylene in aqueous solution under high pressure: 1. Small-angle neutron scattering and densitometric measurements at room temperature. *Polymer* **1987**, *28*, 1738.

(29) Hu, T.; Wu, C. Grafting Density Induced Stretching and Collapse of Tethered Poly(ethylene Oxide) Chains on a Thermally Sensitive Microgel. *Macromolecules* **2001**, *34*, 6802.

(30) Hu, T.; Wu, C. Clustering Induced Collapse of a Polymer Brush. *Phys. Rev. Lett.* **1999**, *83*, 4105.

(31) Pedersen, J. S.; Svaneborg, C. Scattering from block copolymer micelles. *Curr. Opin. Colloid Interface Sci.* **2002**, *7*, 158.

(32) Poppe, A.; Willner, L.; Allgaier, J.; Stellbrink, J.; Richter, D. Structural Investigation of Micelles Formed by an Amphiphilic PEP−PEO Block Copolymer in Water. *Macromolecules* **1997**, *30*, 7462.

(33) Eduljee, H. E.; Newitt, D. M.; Weale, K. E. Pressure−Volume−Temperature Relations in Liquids and Liquid Mixtures. Part I. The Compression of n-Hexane, n-Heptane, n-Octane, and of their Binary and Ternary Mixtures, up to 500 Atmospheres. *J. Chem. Soc.* **1951**, 3086.

Received for review March 14, 2003
Revised manuscript received June 19, 2003
Accepted June 20, 2003

IE0302387